Accurate and comprehensive evaluation of *MGMT* promotor methylation by nanopore sequencing

Skarphedinn Halldorsson [*1], Richard Nagymihaly[1], Areeba Patel [2,3], Petter Brandal[4,6], Ioannis Panagopoulos [4], Henning Leske [5,7], Marius Lund-Iversen[5], Felix Sahm [2,3], and Einar O. Vik-Mo [†1,8]

[1]Vilhelm Magnus Laboratory, Institute for Surgical Research, Department of Neurosurgery, Oslo University Hospital, Oslo, Norway

[2]Department of Neuropathology, University Hospital Heidelberg, Heidelberg, Germany

[3]CCU Neuropathology, German Consortium for Translational Cancer Research (DKTK, German Cancer Research Center (DKFZ), Heidelberg, Germany

[4]Section for Cancer Cytogenetics, Institute for Cancer Genetics and Informatics, Oslo University Hospital

[5]Department of Pathology, Oslo University Hospital, Oslo, Norway.

[6]Department of Oncology, Oslo University Hospital, Oslo, Norway

[7]University of Oslo, Oslo, Norway

[8]Institute for Clinical Medicine, University of Oslo, Oslo, Norway

[*]skarphedinn.halldorsson@rr-research.no
[†]einar.vik-mo@rr-research.no

Abstract

Aims

This study aimed to evaluate the utility of nanopore long-read sequencing as a method for assessing methylation status in the O6-methylguanine-DNA methyltransferase (MGMT) promoter region in glioblastoma (GBM) patients. We sought to compare its performance to conventional techniques and assess its potential for clinical applications.

Methods

We analyzed a total of 165 samples from CNS tumors, focusing on the MGMT CpG island using nanopore sequencing. Oxford Nanopore Technologies (ONT) MinION and PromethION flow cells were employed for single sample or barcoded assays, guided by a CRISPR/Cas9 protocol, adaptive sampling or as part of a whole genome sequencing assay. Methylation data obtained through nanopore sequencing were compared to results obtained via pyrosequencing and methylation bead arrays. Hierarchical clustering was applied to nanopore sequencing data for patient stratification.

Results

Nanopore sequencing displayed a strong correlation (95%) with pyrosequencing results for the four CpGs of MGMT analysed by both methods. The MGMT-STP27 algorithm's classification was effectively reproduced using nanopore data. Unsupervised hierarchical clustering revealed distinct patterns in methylated and unmethylated samples, providing comparable survival prediction capabilities. Nanopore sequencing yielded high-confidence results in a rapid timeframe, typically within hours of sequencing, and extended the analysis to all 98 CpGs of the MGMT CpG island.

Conclusions

This study establishes nanopore sequencing as a valid and efficient method for determining MGMT methylation status in GBM patients. It offers a comprehensive view of the MGMT promoter methylation landscape and the potential to identify clinically relevant subgroups. Further exploration of the clinical implications of patient stratification using nanopore sequencing of MGMT is warranted.

Keywords: *MGMT* promoter methylation, Nanopore sequencing, CRISPR/Cas9, Glioblastoma

Introduction

Glioblastoma (GBM), IDH-wildtype is the most common and most aggressive primary malignant brain tumor in adults [23] with a median survival of about 15 months [31]. Standard treatment for GBM involves surgical resection followed by a combination of radiation and chemotherapy. The frequently used chemotherapeutic drug temozolomide (TMZ) is an alkylating agent that induces methylation of O-6 guanidine residues in dividing cells, leading to DNA damage and apoptosis [38]. Although often well tolerated, TMZ can cause a range of side effects and is therefore suggested to be limited to patients that are likely to benefit from it and withheld from patients that most likely will experience side effects without improvement in survival [14]. The alkylating effects of TMZ are countered by the DNA repair protein O-6-methylguanine-DNA methyltransferase (MGMT). Methylation of the *MGMT* promoter is believed to silence its expression, thereby increasing sensitivity of GBM tumor cells to TMZ [21]. The presence of *MGMT* promoter methylation has been associated with increased survival in GBM patients treated with temozolomide and radiation therapy [13]. *MGMT* promoter methylation status is therefore an important factor for the management and treatment of GBM [6].

Various methods are utilized to directly measure or estimate *MGMT* promoter methylation, including methylation-specific PCR, pyrosequencing, Sanger sequencing or methylation bead array [17, 29]. All of these methods rely on bisulfite conversion of native DNA and PCR amplification prior to analysis and only include a subset of the 98 CpG sites in the CpG island of *MGMT* [20]. For example, the Qiagen *MGMT* pyrosequencing kit, which is widely used in the clinical setting, detects methylation on 4 CpG sites (76-79) in the *MGMT* CpG island. In addition, there is neither a clear consensus on the best cut-off values for the classification of clinically relevant methylated or unmethylated samples, nor on the optimal method to use [3]. In recent years, advances in sequencing technology have enabled more sensitive and accurate detection of DNA methylation. Nanopore sequencing, which uses a nanopore-based sensor to detect changes in electrical current as nucleic acids (DNA or RNA) pass through a pore, can detect epigenetic modifications, such as methylation, directly from the raw current signal [16]. Due to the long-read nature of nanopore sequencing, it also affords methylation analysis of far longer sequences than methylation specific PCR, pyrosequencing or methylation bead array. Consequently, nanopore sequencing offers an overview of the methylation status of all CpGs of the *MGMT* CpG-island, using native genomic DNA without bisulfite conversion, which can be

both time and cost efficient in a clinical setting [18]. Recently developed enrichment methods such as nanopore Cas9 targeted sequencing (nCATs) [8] and adaptive sampling (AS) [25] can be used to direct the sequencing effort to specific genomic regions. In this study, we compared the results of nanopore sequencing of the *MGMT* promoter region of 165 samples from central nervous system (CNS) tumors, including 103 GBMs, with results obtained from standard diagnostic methods such as pyrosequencing or Illumina 850K bead array.

Materials and Methods

Patients and samples

Samples from four independent cohorts were included into this study; 1) Retrospective analysis of DNA from 68 CNS tumor samples provided by the Institute for Cancer Genetics and Informatics, Oslo University Hospital that were screened for *MGMT* promoter methylation using the Qiagen® *MGMT* pyrosequencing kit (MGMT pyro kit). These samples are referred to as "Retrospective nCATs". 2) Retrospective analysis of 67 sequences generated as part of the Rapid-CNS adaptive sampling pipeline [24] analyzed by Illumina® methylation 850K bead array. These samples are referred to as "Rapid-CNS". 3) DNA extracted from 16 glioma biopsies from patients operated at Oslo University Hospital. A separate biopsy derived from paraffin-embedded tissue was analysed with the Qiagen® *MGMT* pyrosequencing kit at the Department of Molecular Pathology. These samples are referred to as "Prospective nCATs". 4) DNA from 18 CNS tumors was extracted and sequenced in total as part of a whole geneome sequecing project. These samples are referred to as "WGSeq". Supplementary Table 1 provides an overview of all samples used in this study. Written, informed consent was obtained from patients at the time of surgery and reviewed by the ethical review board at the respective institutions. Samples were collected through both new and previously published studies and approved according to Regional ethical board number S-06046, 2016/1791, and 388359 [24].

In total, 165 samples were analyzed for *MGMT* promoter methylation status, including 103 GBM samples and 28 IDH-mutant glioma samples. Figure 1b shows distribution of sample classification and predetermined methylation status. Two methods were used to enrich for the region of interest: CRISPR/Cas9 targeted sequencing of the *MGMT* promoter region [35] and adaptive sampling. Cas9 targeted sequencing was applied to 81 sample, 45 of which were run as single samples and 36 were run as multiplexed groups of five. 67 samples were previously analyzed

as part of an adaptive sampling pipeline. The remaining 18 samples were analyzed as part of a whole genome sequencing panel.

Sample preparation and nanopore sequencing

Between 10 and 25 mg of fresh/frozen tissue were used to extract genomic DNA (Merck's GenElute™ Mammalian Genomic DNA Miniprep kit) following the manufacturer's protocol. Purity and concentration of DNA samples was determined using NanoDrop™ One and Qubit™ 4 Fluorometers (Thermo Fischer Scientific).

nCATs

Cas9 mediated targeted sequencing was performed with the Cas9 Sequencing Kit (Oxford Nanopore Technologies) according to the manufacturers protocol (version ENR 9084 v109 revR 04Dec2018). Briefly, Cas9 ribonucleoprotein complexes (RNPs) were created by mixing equimolar concentrations (100 µM) of crispr RNA (crRNA) and trans-activating elements (tracrRNA) to HiFi Cas9 enzyme (IDT). Dephosphorylated gDNA (2-5 µg) was cleaved and dA-tailed with Cas9 RNPs and Taq polymerase. Finally, sequencing adaptors were ligated to the cleaved fragments and the final DNA library was purified with AMPure XP beads (Beckman Coulter). Barcodes were applied to a number of samples to allow multiplexing of five samples based on an experimental protocol from Oxford Nanopore Technologies (UNPUBLISHED Cas9 Native Barcoding, version: cas-native-barcoding-v1-revA). Purified DNA libraries were loaded onto R9.4.1. flow cells on MinION Mk1B or Mk1C devices and sequenced for 4-24 hours. Individual flow cells were flushed and re-used up to four times for single samples and twice for multiplexed samples. A minimum pore-count of 300 was deemed sufficient for a single sample, 800 for multiplexed samples.

Whole genome sequencing

Whole genome sequnecing of CNS tumor DNA was performed by with the Ligation sequencing kit SQK-LSK114 and protocol (version: sqk-lsk114 GDH 9173 v114 revH 10Nov2022 promethion) from ONT. Libraries were loaded onto R10.4.1 PromethION flow-cells (one sample per flow-cell) and sequenced for 72 hours.

RAPID-CNS

Raw fast5 sequences of all fragments mapping to the *MGMT* promoter in the Rapid-CNS [24] data were provided for re-analysis.

Primers

All primers were purchased from Integrated DNA Technologies (Leuven, Belgium). Previously published primers were initially used to target the *MGMT* promoter [35], termed MGMT-left-1 (ATGAGGGGCCCACTAATTGA) and MGMT-right-1 (ACCTGAGTATAGCTCCGTAC), yielding a fragment of 2,522 bp. In order to increase cas9 efficiency and expand the size of the fragment, we added additional crRNA primers: MGMT-left-2 (GCCAACCACGTTAGAGACAATGG), MGMT-right-2 (GTACGGAGCTATACTCAGGT), MGMT-right3 (CTGGAATCGCATTCCAGTAGTGG) and MGMT-right-4 (ACTTCGCAAGCATCACAGGTAGG) resulting in a fragment of 4,800 bp.

Data analysis

Raw sequences were basecalled, methylation called and mapped (hg38, chromosome 10) using the Guppy toolbox (version 6.4.6) from ONT. Per site methylation values were extracted from modified BAM files and aggregated across forward and reverse strands using the modkit toolbox (version 0.2.2) from ONT. All statistical analyses were performed in R (version 4.2.1). The source code and data to reproduce all analyses and figures from this manuscript is available at https://github.com/SkabbiVML/MGMT_R.

Results

Data acquisition

Sequence depth of the *MGMT* promoter region in the samples varied based on method, sequencing time as well as DNA and flow-cell quality. This is reflected in the per site valid methylation coverage (methylated bases + canonical bases). Single sample runs produced on average more sequences in the region of interest and higher mean methylation coverage (mean = 69.4, median = 28.1) than barcoded runs (mean = 13.6, median = 10.3) and adaptive sampling (mean = 12.2, median = 9.8) (Figure 1c). No bias in sequencing depth was observed between methylated and unmethylated samples across Cas9 targeted or WGS samples, either single or multiplexed.

However, a statistically significant difference in methylation coverage was observed between methylated (mean = 15.9, median = 16.2) and unmethylated (mean = 10.5, median = 10.6) samples analyzed by adaptive sampling (p=0.012).

Nanopore sequencing compared to established methods

The MGMT pyro kit and the *MGMT*-STP27 classifier are common methods to infer the clinically relevant methylation status of the *MGMT* promoter region. Both of these methods rely on a limited number of CpG sites. A subset of our samples ("Retrospective nCATs", n=68) were previously analyzed using the Qiagen® *MGMT* pyrosequencing kit (MGMT pyro kit), which specifically measures CG methylation on four CpG sites in Chr10:129467253-129467272 (hg38) which corresponds to CpGs 76-79 of *MGMT* promoter CpG island. To directly compare the results of nanopore sequencing and the MGMT pyro kit, we extracted methylation results for CpGs 76-79 from the nanopore data and compared them to methylation values obtained using the MGMT Pyro kit (Figure 2). Pearson's correlation coefficient between the methylation values of each overlapping CpG site between nanopore and pyrosequencing ranged from 0.89 to 0.94 (R^2 = 0.79-0.89) (Figure 2a). Results from the MGMT pyro kit are typically returned as an average methylation percentage of all four CpGs for classification and clinical decision making. When results of nanopore sequencing and the MGMT Pyro kit are averaged across all four CpG sites, the correlation increased to 0.95 (R^2 = 0.91) (Figure 2b).

An average methylation level of $\geq$ 10% using the MGMT pyro kit is considered to be methylated [17, 26]. To compare classification results of nanopore sequencing and the MGMT pyro kit, a logistic regression model was trained using the average methylation of CpGs 76-79 based on nanopore sequencing and classification based on the MGMT pyro kit as the indicator. An ROC curve of the fitted model showed an AUC of 0.992 (Figure 2c). The optimal methylation percentage by nanopore sequencing to separate methylated and unmethylated samples as classified by MGMT pyro kit was 22% methylated (95% confidence intervals <10% and >33% methylated). Applying this logistic regression model to the remaining samples to predict methylation status showed reduced sensitivity and specificity with an AUC of 0.951. Two of 62 samples (3.2%) in the training set (Retrospective nCATs) were misclassified while 12 of the 98 remaining samples (12.2%) were misclassified (Figure 2d).

Illumina® Human Methylation BeadChips (HM-27K, HM-450K, and HM-850K) are microarray-

based platforms used to investigate DNA methylation patterns in human samples. These platforms only cover a subset of the approximately 30 million CpG sites in the human genome. To predict the clinically relevant methylation status of the *MGMT* promoter, a regression model, *MGMT STP27*, has been developed. This model uses the methylation status of two array probes, cg12434587 (CpG 31) and cg12981137 (CpG 84), as reported by Bady *et al.* [2, 1].

The samples from the Rapid-CNS study (n=67) were analyzed by Illumina® HM-850K EPIC array in addition to nanopore sequencing and the ground truth methylation status was derived from the *MGMT*-STP27 classifier. To compare nanopore sequencing results to the *MGMT*-STP27 classifier results, the methylation level of the two CpG sites represented in the *MGMT*-STP27 algorithm were extracted and the methylation percentage values were plotted against each other (Figure 3a). The unmethylated samples generally show low methylation on both sites while methylated samples display a varied degree of methylation on both sites. A multiple logistic regression model based on the methylation percentage of CpG 31 and and CpG 84 in the Rapid-CNS data with known status as the indicator was generated. AUC of the training model was 0.972. (Figure 3b). The model accurately predicted the *MGMT* known methylation status of 77 of the remaining 97 samples (80%) with an AUC of 0.944.
Taken together, nanopore sequencing of the *MGMT* promoter region can be used to recreate methylation status classification of either the MGMT pyro kit or methylation bead array and the *MGMT*-STP27 classifier with high accuracy.

Clustering based on nanopore sequencing separates methylated and unmethylated samples

To investigate the impact of methylation at all CpG sites within the *MGMT* promoter CpG island, we compared the average methylation of each CpG site between methylated and unmethylated samples (Figure 4a). The average methylation percentage of each CpG site in methylated and unmethylated samples showed that the biggest differences in methylation levels to occur at CpGs 7 through 14 and 72 through 91. Welch's two sided t-tests between methylated and unmethylated samples were performed at every CpG site and the results adjusted for multiple testing (Bonferroni method). Figure 4b shows the adjusted p-values for every site in the *MGMT* CpG island. Interestingly, low p-values were observed at CpG sites 4 through 14 (excluding CpG 7) which are far upstream of DMR1 and DMR2 (Figure 1a). Furthermore, 19 CpG sites were

found to have lower p-values when comparing methylated and unmethylated samples than the CpG sites included in the MGMT pyro kit (CpGs 76-79) or the *MGMT*-STP27 classifier (CpGs 31 and 84) Figure 4b. Unsupervised hierarchical clustering based on all 98 CpG sites of the CpG island using Ward's method reveals two main clusters that largely correspond to the previously determined classification (Figure 4c).

Unmethylated samples exhibited low methylation levels throughout the CpG island, except for the first 5 CpG sites, which were often methylated regardless of overall methylation status of the sample. In contrast, methylated samples showed a larger gradient of methylation, with higher levels of methylation towards either end of the CpG island.

Clustering based on nanopore sequencing categorized nine samples previously classified as methylated with otherwise unmethylated samples and seven unmethylated samples with otherwise methylated samples (Figure 4c). This pattern of separation is also evident when unsupervised clustering was performed on GBM samples only (Figure 5a).

Survival analysis of GBM patients based on nanopore sequencing

While clustering based on nanopore methylation profiles were largely in agreement with classification based on established methods, discrepancies were also observed (Figure 4c and Figure 4c). Therefore, we investigated whether clustering by nanopore sequencing was comparable to established methods in predicting patient survival. We performed survival analysis on 30 GBM patients under 75 years of age (11 females, average age 58.4 years and 19 males, average age 60.2 years) treated at Oslo University hospital by surgery followed by radiotherapy combined with concomitant and adjuvant temozolomide. Biopsies were analyzed by both MGMT pyro kit and nanopore sequencing (Table 1). Patients were classified as methylated or unmethylated based on the 10% cut-off value by the MGMT pyro kit or placement within the two major clusters by hierarchical clustering of nanopore sequencing data Figure 5a.

Kaplan-Meier survival analysis of patients based on the MGMT pyro kit showed longer median survival of patients classified as methylated compared to patients classified as unmethylated (Figure 5b, 23.8 months vs. 20.9 months). However, the difference in survival did not reach statistical significance (p=0.81). When patients were classified according to clustering of nanopore sequencing data, significantly longer survival was observed in "Cluster 2" patients compared to "Cluster 1" patients (Figure 5c, 24.5 months vs. 21.1 months, p=0.0039). Clusters 1 and 2 largely represent unmethylated and methylated patients, respectively, with some exceptions.

Discussion

Ever since *MGMT* promoter methylation was discovered as a prognostic marker for over-all and progression-free survival in GBM [12, 7], there has been an ongoing debate regarding the optimal method and optimal cut-off to determine clinically relevant methylation of the *MGMT* promoter (Supplementary Table 2). Methylation-specific PCR, pyrosequencing and methylation bead arrays are commonly used to determine *MGMT* methylation status, but when these methods have been directly compared, results have been discordant in up to a third of cases [32, 11, 17]. This is likely due to lack of consensus between CpG sites queried by different methods and different cut-offs applied. A recent meta-analysis including 32 cohorts and 3474 patients could not draw strong conclusions of the optimal CpG sites to query and optimal cut-off to apply [3]. This underlines the need for thorough method validation by every institution on their own patient cohort. Considerable effort has been put into finding a minimal set of CpG sites within the *MGMT* CpG island that can best predict *MGMT* expression and/or patient survival [1, 17, 4, 28, 30, 19]. This is partially due to the necessity to provide simplified assays that fit the short-read framework of bisulfite sequencing techniques. Most, if not all, clinically established methods of *MGMT* methylation classification, such as methylation specific PCR, quantitative methylation specific PCR, MGMT pyro kit or the *MGMT* SPT27 classifier, rely on the methylation status of very limited number of CpG sites to predict the methylation status of the whole promoter. Although these assays have been shown to largely agree on highly methylated or completely unmethylated samples, they are less reliable when it comes to moderately methylated or 'grey-zone' samples [33].

Analysis of *MGMT* promoter methylation by nanopore sequencing has several advantages over conventional techniques. First, nanopore sequencing can detect epigenetic modifications on native DNA, thereby circumventing the need for bisulfite treatment. This saves time and reduces the potential risk of bias introduced by bisulfite treatment and PCR that has been shown to underrepresent densely hydroxymethylated (5hmC) regions [15]. Using native DNA without manipulation or amplification minimizes this bias and reduces the risk of bias between sequencing data generated by different laboratories. Secondly, the long-read nature of nanopore sequencing offers a complete overview of methylation of the region of interest and can be extended in either direction to include the shores and shelves of the CpG island. Regions outside the DMR2 are neglected by most established assays but have been shown to discriminate the

methylation status of GBMs [32]. Third, the flexibility of nanopore sequencing makes it possible to incorporate *MGMT* methylation analysis to assays such as whole genome sequencing, exome sequencing, *in silico* enrichment (adaptive sampling) or cas9 targeted enrichment, either as single samples or multiplexed. Finally, the up-front cost of nanopore sequencing is low compared to other sequencing techniques and can be established by smaller laboratories or clinics.

In this study we analyzed 165 CNS tumor samples using targeted or whole genome nanopore sequencing and compared the results to those acquired by pyrosequencing and methylation bead arrays. We reported 95% correlation between nanopore sequencing of the four CpG sites analyzed by the MGMT-pyro kit and established an optimal cut-off for nanopore sequencing of the same CpG sites to recreate the pyrosequencing results with 97% accuracy. We also recreated sample classification via methylation bead array and the *MGMT*-STP27 classifier with nanopore sequencing data with 91% accuracy. In addition, nanopore sequencing allowed expansion of the area of analysis to include all 98 CpGs of the *MGMT* CpG island as previously proposed to be critical for MGMT expression [21]. Unsupervised hierarchical clustering of samples based on nanopore methylation data of the *MGMT* CpG island showed clear separation into groups that largely correspond to methylated and unmethylated samples. Finally, we showed that patient survival prediction based on clustering of nanopore sequencing data was comparable, if not superior, to classification via the MGMT Pyro kit. To the best of our knowledge, this is the first study to examine all 98 CpG sites within the *MGMT* CpG island in multiple patient biopsies by nanopore sequencing.

The results presented here demonstrate that nanopore sequencing of the *MGMT* promoter region can largely recreate the results of established bisulfite dependant methods while providing additional data on epigenetic regulation of *MGMT* and may provide novel criteria for patient stratification. Although the sample size is small, our results suggest that classifying patients via nanopore sequencing is as reliable as classification with methods such as the MGMT pyro kit or methylation bead arrays. Unsupervised hierarchical clustering of glioblastoma samples based on nanopore sequencing indicates the presence of one or more sub-groups within the previously defined methylated samples. These groups are defined by both extent and level of methylation. Further studies and larger patient cohorts are needed to elucidate the functional implications of these sub-groups.

The study is not without limitations. Although 165 patients were included for the evaluation of nanopore sequencing as a method to analyse *MGMT* CpG island methylation, only 103 samples were from diagnosed GBM patients and survival data from primary GBM patients was only available for 30 patients. This limited our ability to evaluate survival beyond the major groups. Our data do not include estimation of tumor-cell content in the biopsies and do not take into account the possibilities of tumor heterogeneity for *MGMT* promoter methylation, which has previously been shown to affect some gliomas [34]. While the clustering of nanopore sequencing data effectively distinguished between methylated and unmethylated samples, notable discordances emerged when compared to results obtained through conventional methods. This discrepancy underscores the existing uncertainties inherent in the current classification of *MGMT* methylation status and highlights the need for additional investigations. The remarkable granularity of nanopore data offers a promising foundation for refining classification, especially in borderline cases. Future studies leveraging the nuanced information provided by nanopore sequencing have the potential to enhance the accuracy and reliability of *MGMT* methylation status determination.

We conclude that methylation status evaluation by nanopore sequencing of the *MGMT* promoter region is comparable to established methods while providing considerable additional information. This is true for both cas9 targeted sequencing of the *MGMT* CpG island and inclusion of the *MGMT* promoter region into an adaptive sequencing panel or whole genome sewuencing. Distinct subgroups within methylated samples were observed via nanopore sequencing although any difference in patient outcome between these clusters has yet to be determined.

Acknowledgements

The authors would like to thank the patients who participated in this study and their families. We also thank Dr. Thidathip Wongsurawat for sharing her knowledge on Cas9 targeted sequencing and primer sequences. This project was funded through generous grants from The Regional Health authorities HSØ #20170073, #20210039, and #20230059.

Tables

Table 1: Patients used in survival analysis

Age	Sex	Diagnosis	IDH	Resection	Treatment	OS (months)	Status	*MGMT* Status (Pyro)	Nanopore cluster
66	F	GBM	Neg	GTR	Stupp	14.99	Dead	Unmethylated	1
78	M	GBM	Neg	GTR	Stupp	5.19	Dead	Methylated	2
58	M	GBM	Neg	STR	Stupp	24.5	Dead	Methylated	2
57	F	GBM	Neg	STR	Stupp	28.77	Dead	Methylated	2
73	M	GBM	Neg	STR	Stupp	20.91	Dead	Unmethylated	1
77	M	GBM	Neg	STR	Stupp	11.97	Dead	Unmethylated	1
60	M	GBM	Neg	GTR	Stupp	29.26	Dead	Methylated	2
65	M	GBM	Neg	STR	Stupp	29.69	Dead	Methylated	2
62	F	GBM	Neg	STR	Stupp	6.9	Dead	Unmethylated	1
64	M	GBM	Neg	STR	Stupp	25.48	Dead	Methylated	2
58	M	GBM	Neg	STR	Stupp	21.6	Dead	Methylated	2
58	M	GBM	Neg	STR	Stupp	11.44	Dead	Unmethylated	1
72	F	GBM	Neg	STR	Stupp	21.21	Dead	Methylated	2
58	F	GBM	Neg	STR	Stupp	13.61	Dead	Methylated	2
66	M	GBM	Neg	STR	Stupp	21.96	Dead	Methylated	2
51	M	GBM	Neg	GTR	Stupp	12.85	Dead	Methylated	2
64	F	GBM	Neg	STR	Stupp	8.3	Dead	Methylated	1
52	F	GBM	Neg	STR	Stupp	23	Dead	Methylated	2
66	F	GBM	Neg	STR	Stupp	13.6	Dead	Methylated	2
49	M	GBM	Neg	GTR	Stupp	9.4	Dead	Unmethylated	1
46	F	GBM	Neg	GTR	Stupp	14.31	Alive	Methylated	2
60	F	GBM	Neg	GTR	Stupp	14.08	Alive	Methylated	1
55	M	GBM	Neg	GTR	Stupp	15.16	Alive	Unmethylated	2
66	M	GBM	Neg	GTR	Stupp	14.47	Alive	Methylated	2
39	F	GBM	Neg	GTR	Stupp	13.78	Alive	Methylated	1

Figures

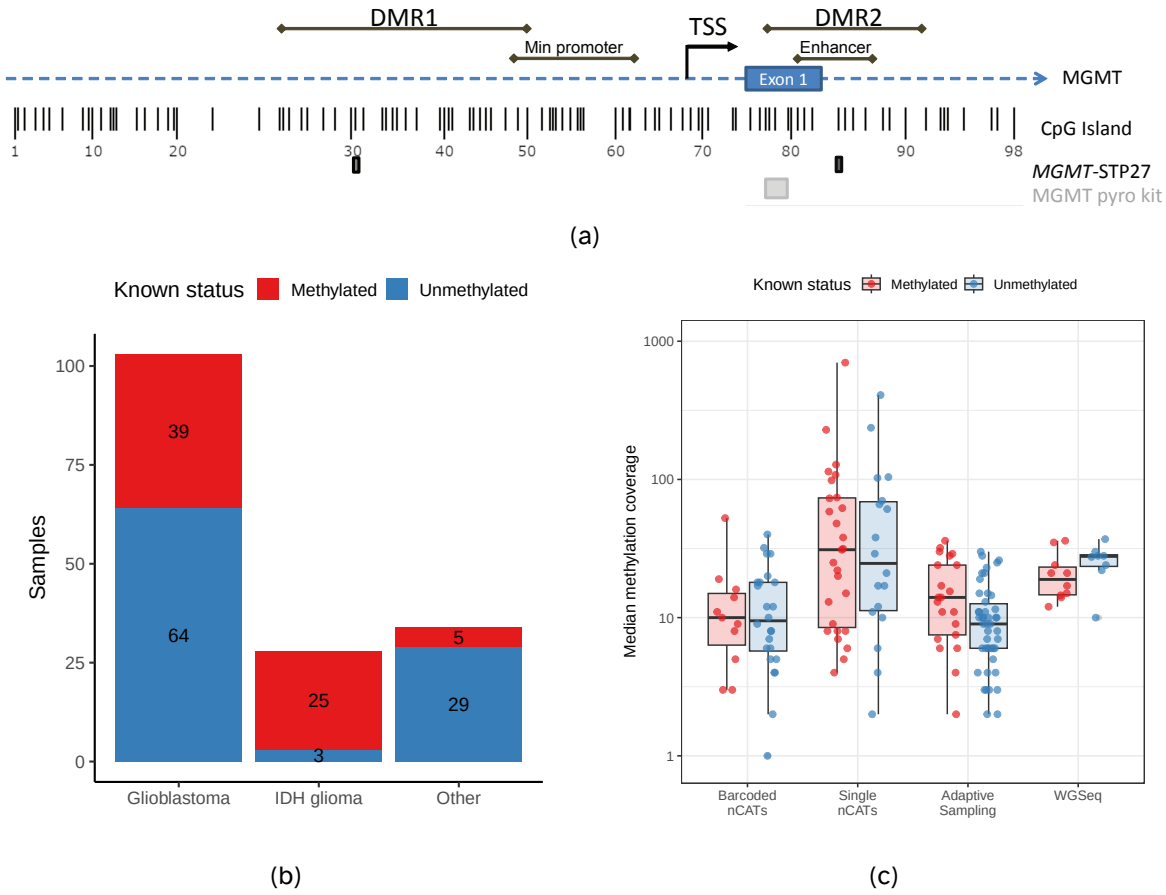

Figure 1: (a) Schematic overview of the 98 CpG sites of the *MGMT* promoter CpG island with relevant functional areas including the transcription start site (TSS), minimal promoter and enhancer as defined by Harris *et al.* [9, 10] as well as the differentially methylated regions (DMR) one and two as described by Malley *et al.* [20]. The two CpG sites used by the *MGMT*-STP27 classifier [2] and the four CpG sites included in the Qiagen® *MGMT* pyrosequencing kit are shown below. (b) Distribution of diagnosis and known methylation status of the sample cohort. (c) Median methylation coverage of the 98 CpG sites in the *MGMT* promoter region of methylated and unmethylated samples by method of acquisition (Adaptive sampling, multiplexed nCats, single sample nCats and whole genome sequencing).

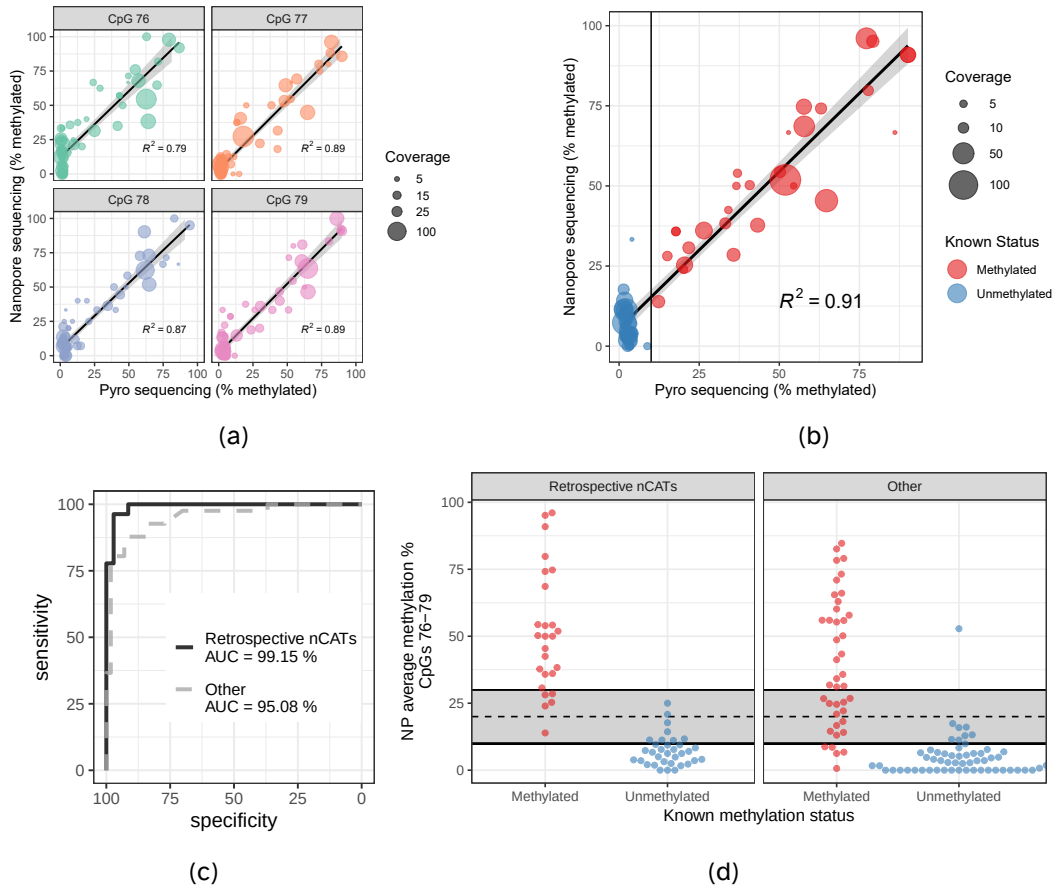

Figure 2: Comparison of nanopore sequencing and Qiagen® MGMT pyro kit of CpGs 76-79 in the *MGMT* CpG island. Results show per-site methylation percentage of each CpG (a) or average values of 4 CpG sites analyzed by the MGMT pyro kit (b) in the "retrospective nCATs" samples. Black vertical line marks the 10 % cut-off value between methylated and unmethylated samples as measured by the MGMT pyro kit. (c) ROC curves for a logistic regression model based on average methylation of CpGs 76-79 by nanopore sequencing (Retrispective nCATs, 62 samples) with classification by the MGMT pyro kit as operator (solid black) and prediction of MGMT status of 98 samples (dashed grey). (d) Comparison of known *MGMT* status (methylated or unmethylated, x-axis) based on the optimal average methylation threshold of CpGs 76-79 derived from the training samples (retrospective nCATs, left) and model predictions (other samples, right). The Y-axis represents average methylation percentage of CpG sites 76-79 based on nanopore sequencing. Dashed horizontal line represents the optimal threshold of 22% methylated, grey box represents 95% confidence interval (<10% and >33%)

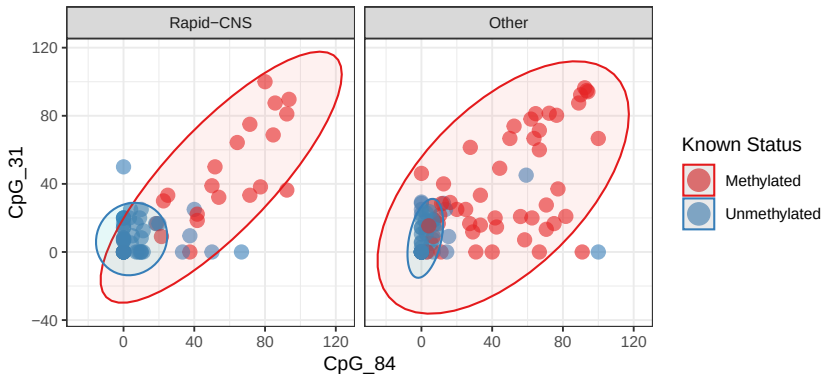

(a)

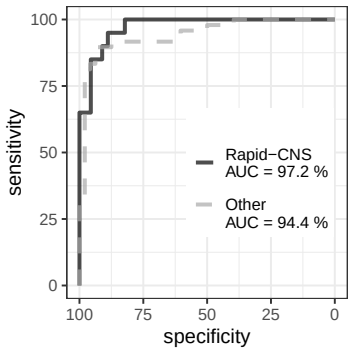

(b)

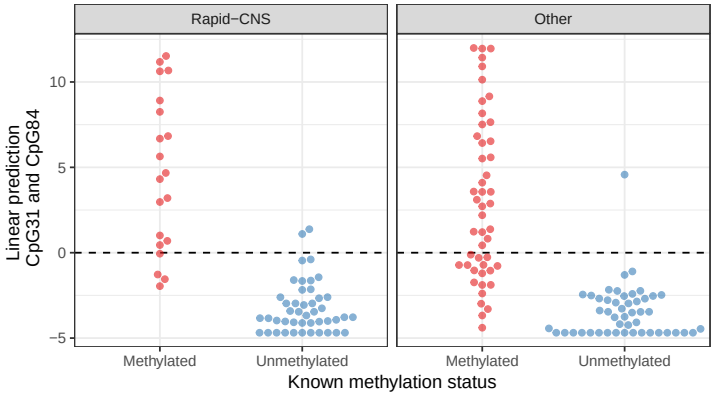

(c)

Figure 3: Comparison of nanopore sequencing and the *MGMT*-STP27 classifier. (a) Methylation percentage of CpG 31 (probe ID: cg12434587) and CpG 84 (probe ID: cg12981137) in the *MGMT* promoter for the 67 samples in the Rapid-CNS cohort (left) and remaining samples (right). Elipses represent 90% confidence intervals. (b) ROC curves for a logistic regression model based on methylation of CpGs 31 and 84 by nanopore sequencing (Rapid-CNS) with classification by the *MGMT*-STP27 classifier as operator (solid black) and prediction of MGMT status of remaining 99 samples (dashed grey). (c) Separation of samples based on the linear predictors extracted from the logistic regression model.

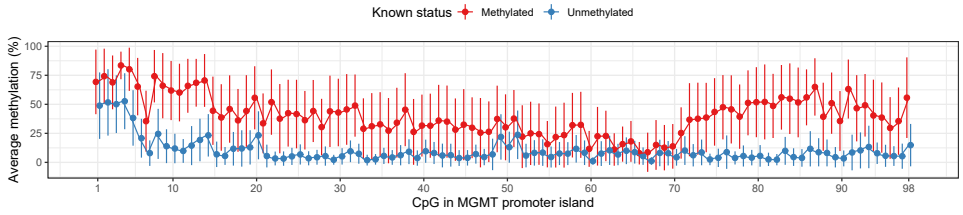

(a)

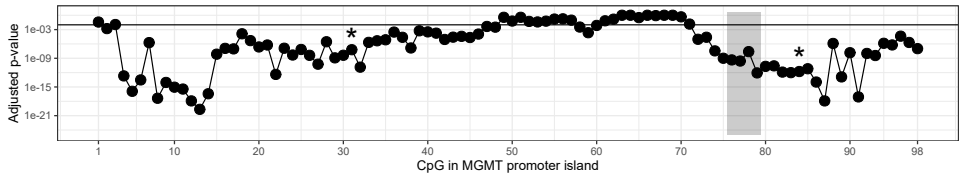

(b)

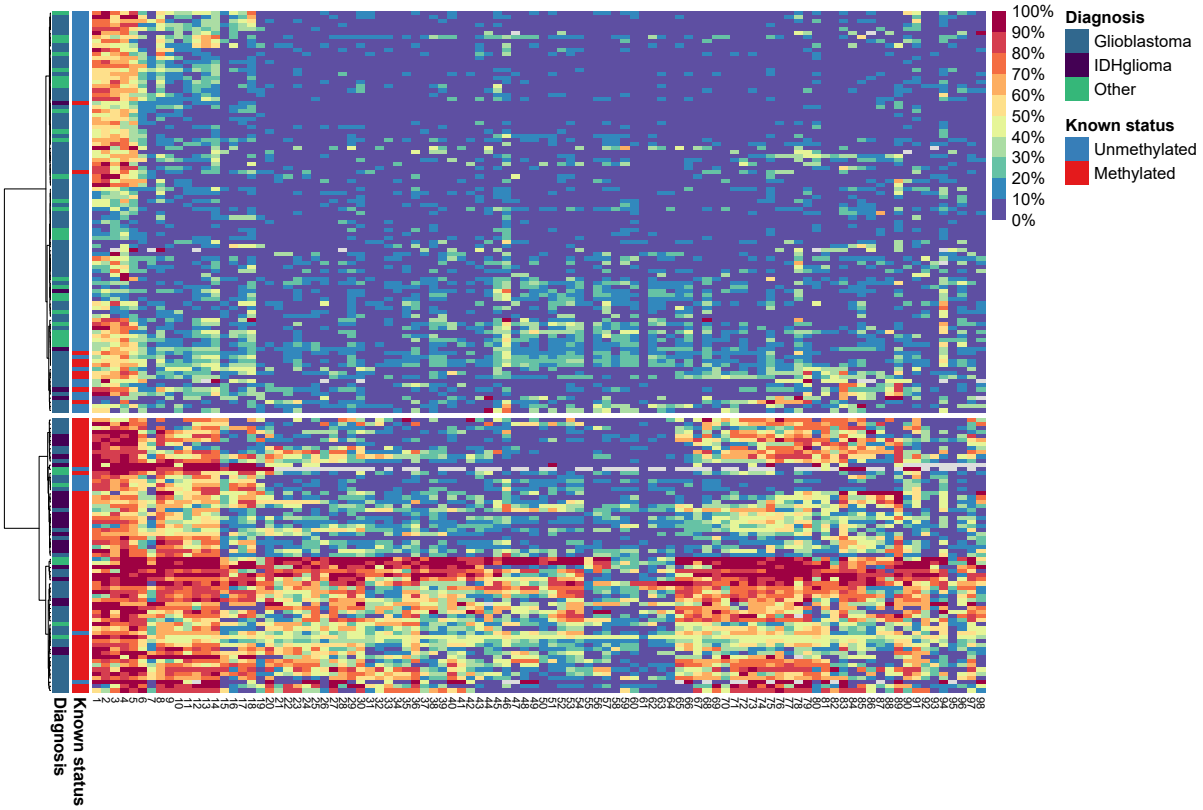

(c)

Figure 4: (a) Dotplot showing average methylation percentage of each CpG site in the *MGMT* CpG island. Error bars represent standard deviation. (b) Dotplot showing Bonferroni adjusted p-values of Welch's two-sided t-test between methylated and unmethylated samples for each CpG site. Grey vertical bar shows the location of CpG sites analyzed by the MGMT pyro kit, asterixes show the location of probes included in the *MGMT*-STP27 classifier. Horizontal line depicts 0.01. (c) Unsupervised hierarchical clustering of all samples based on nanopore sequencing of 98 CpG sites of the *MGMT* promoter CpG island (n = 165).

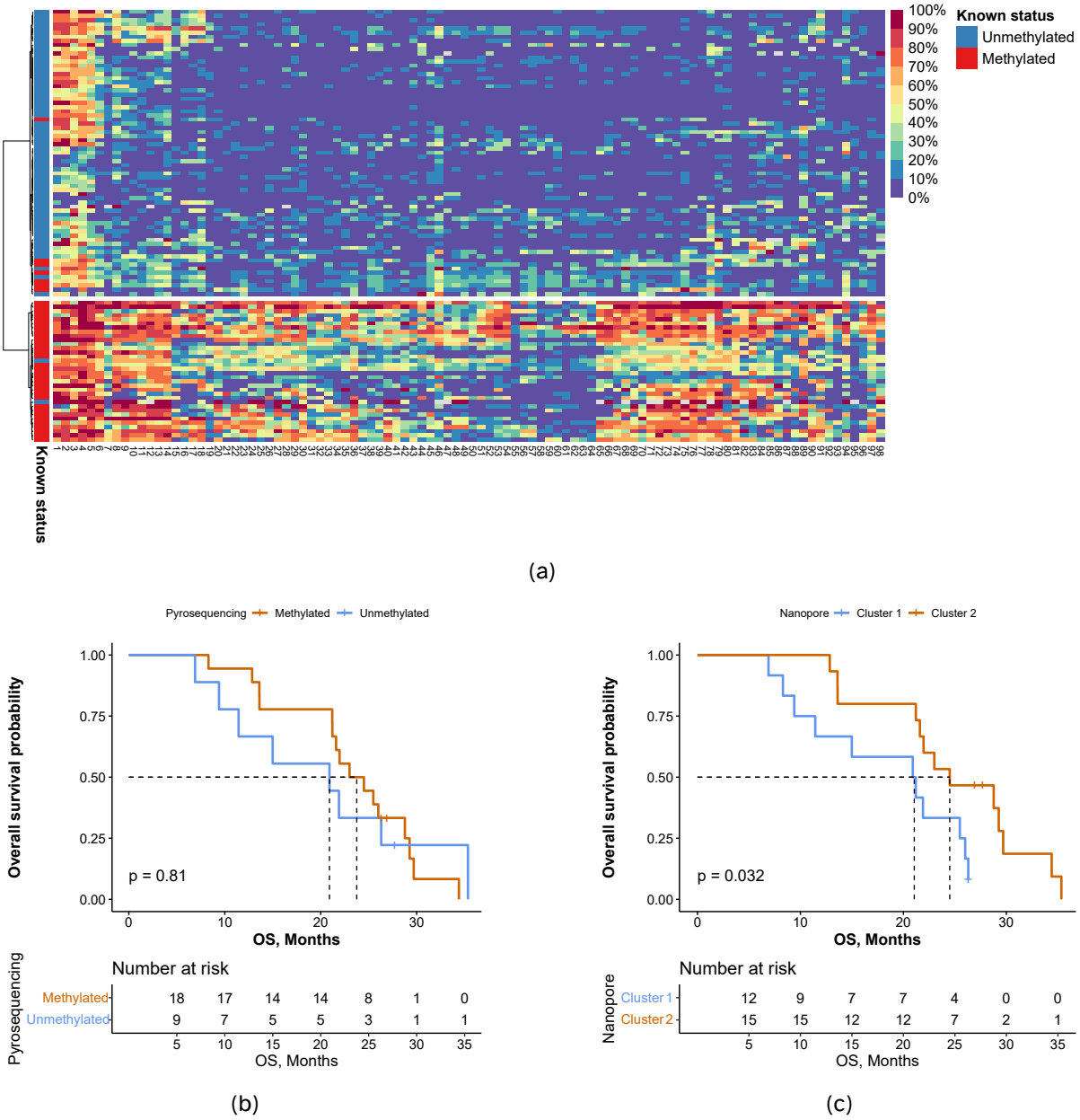

Figure 5: (a) Heatmap showing unsupervised clustering of all glioblastoma samples based on nanopore sequencing of the *MGMT* promoter (n = 103). Kaplan-Meier patient survival curves based on (b) MGMT pyro kit classification or (c) hierarchical clustering according to nanopore sequencing in Figure 5a . Dotted lines represent group median survival (Pyrosequencing-methylated = 22.5 months, Pyrosequencing-unmethylated = 17.9 months, Nanopore-Cluster1 = 20.9 months, Nanopore Cluster2 = 23.0 months).

References

[1] Bady, P., Delorenzi, M., and Hegi, M. E. Sensitivity Analysis of the MGMT-STP27 Model and Impact of Genetic and Epigenetic Context to Predict the MGMT Methylation Status in Gliomas and Other Tumors. *Journal of Molecular Diagnostics 18*, 3 (2016).

[2] Bady, P., Sciuscio, D., Diserens, A. C., Bloch, J., Van Den Bent, M. J., Marosi, C., Dietrich, P. Y., Weller, M., Mariani, L., Heppner, F. L., Mcdonald, D. R., Lacombe, D., Stupp, R., Delorenzi, M., and Hegi, M. E. MGMT methylation analysis of glioblastoma on the Infinium methylation BeadChip identifies two distinct CpG regions associated with gene silencing and outcome, yielding a prediction model for comparisons across datasets, tumor grades, and CIMP-status. *Acta neuropathologica 124*, 4 (2012), 547–560.

[3] Brandner, S., McAleenan, A., Kelly, C., Spiga, F., Cheng, H. Y., Dawson, S., Schmidt, L., Faulkner, C. L., Wragg, C., Jefferies, S., Higgins, J. P., and Kurian, K. M. MGMT promoter methylation testing to predict overall survival in people with glioblastoma treated with temozolomide: A comprehensive meta-analysis based on a Cochrane Systematic Review. *Neuro-Oncology 23*, 9 (9 2021), 1457–1469.

[4] Brigliadori, G., Foca, F., Dall'Agata, M., Rengucci, C., Melegari, E., Cerasoli, S., Amadori, D., Calistri, D., and Faedi, M. Defining the cutoff value of MGMT gene promoter methylation and its predictive capacity in glioblastoma. *Journal of Neuro-Oncology 128*, 2 (2016).

[5] Choi, H. J., Choi, S. H., You, S. H., Yoo, R. E., Kang, K. M., Yun, T. J., Kim, J. H., Sohn, C. H., Park, C. K., and Park, S. H. MGMT promoter methylation status in initial and recurrent glioblastoma: Correlation study with DWI and DSC PWI features. *American Journal of Neuroradiology 42*, 5 (2021).

[6] Christmann, M., Verbeek, B., Roos, W. P., and Kaina, B. O6-Methylguanine-DNA methyltransferase (MGMT) in normal tissues and tumors: Enzyme activity, promoter methylation and immunohistochemistry. *Biochimica et Biophysica Acta (BBA) - Reviews on Cancer 1816*, 2 (12 2011), 179–190.

[7] Dovek, L., Nguyen, N. T., Ozer, B. H., Li, N., Elashoff, R. M., Green, R. M., Liau, L., Leia Nghiemphu, P., Cloughesy, T. F., and Lai, A. Correlation of commercially available quantitative MGMT (O-6-methylguanine-DNA methyltransferase) promoter methylation scores and GBM patient survival. *Neuro-Oncology Practice 6*, 3 (2019).

[8] Gilpatrick, T., Lee, I., Graham, J. E., Raimondeau, E., Bowen, R., Heron, A., Downs, B., Sukumar, S., Sedlazeck, F. J., and Timp, W. Targeted nanopore sequencing with Cas9-guided adapter ligation. *Nature biotechnology 38*, 4 (4 2020), 433–438.

[9] Harris, L. C., Potter, P. M., Tano, K., Shiota, S., Mitra, S., and Brent, T. P. Characterization of the promoter region of the human O6-methylguanine-DNA methyltransferase gene. *Nucleic Acids Research 19*, 22 (1991).

[10] Harris, L. C., Remack, J. S., and Brent, T. P. Identification of a 59 bp enhancer located at the first exon/intron boundary of the human O6-methylguanine DNA methyltransferease gene. *Nucleic Acids Research 22*, 22 (1994).

[11] Håvik, A. B., Brandal, P., Honne, H., Dahlback, H. S. S., Scheie, D., Hektoen, M., Meling, T. R., Helseth, E., Heim, S., Lothe, R. A., and Lind, G. E. MGMT promoter methylation in gliomas-assessment by pyrosequencing and quantitative methylation-specific PCR. *Journal of Translational Medicine 10*, 1 (3 2012).

[12] Hegi, M. E., Diserens, A.-C., Gorlia, T., Hamou, M.-F., de Tribolet, N., Weller, M., Kros, J. M., Hainfellner, J. A., Mason, W., Mariani, L., Bromberg, J. E., Hau, P., Mirimanoff, R. O., Cairncross, J. G., Janzer, R. C., and Stupp, R. MGMT Gene Silencing and Benefit from Temozolomide in Glioblastoma . *New England Journal of Medicine 352*, 10 (2005).

[13] Hegi, M. E., Genbrugge, E., Gorlia, T., Stupp, R., Gilbert, M. R., Chinot, O. L., Burt Nabors, L., Jones, G., Van Criekinge, W., Straub, J., and Weller, M. MGMT promoter methylation cutoff with safety margin for selecting glioblastoma patients into trials omitting temozolomide: A pooled analysis of four clinical trials. *Clinical Cancer Research 25*, 6 (2019), 1809–1816.

[14] Hegi, M. E., and Ichimura, K. MGMT testing always worth an emotion. *Neuro-Oncology 23*, 9 (9 2021), 1417.

[15] Huang, Y., Pastor, W. A., Shen, Y., Tahiliani, M., Liu, D. R., and Rao, A. The behaviour of 5-hydroxymethylcytosine in bisulfite sequencing. *PLoS ONE 5*, 1 (1 2010).

[16] Jain, M., Olsen, H. E., Paten, B., and Akeson, M. The Oxford Nanopore MinION: Delivery of nanopore sequencing to the genomics community. *Genome Biology 17*, 1 (2016).

[17] Johannessen, L. E., Brandal, P., Myklebust, T. Å., Heim, S., Micci, F., and Panagopoulos, I. MGMT gene promoter methylation status – Assessment of two pyrosequencing kits and three methylation-specific PCR methods for their predictive capacity in glioblastomas. *Cancer Genomics and Proteomics 15*, 6 (11 2018), 437–446.

[18] Laver, T., Harrison, J., O'Neill, P. A., Moore, K., Farbos, A., Paszkiewicz, K., and Studholme, D. J. Assessing the performance of the Oxford Nanopore Technologies MinION. *Biomolecular Detection and Quantification 3* (2015).

[19] Leske, H., Camenisch Gross, U., Hofer, S., Neidert, M. C., Leske, S., Weller, M., Lehnick, D., and Rushing, E. J. MGMT methylation pattern of long-term and short-term survivors of glioblastoma reveals CpGs of the enhancer region to be of high prognostic value. *Acta neuropathologica communications 11*, 1 (12 2023).

[20] Malley, D. S., Hamoudi, R. A., Kocialkowski, S., Pearson, D. M., Collins, V. P., and Ichimura, K. A distinct region of the MGMT CpG island critical for transcriptional regulation is preferentially methylated in glioblastoma cells and xenografts. *Acta Neuropathologica 121*, 5 (2011).

[21] Nakagawachi, T., Soejima, H., Urano, T., Zhao, W., Higashimoto, K., Satoh, Y., Matsukura, S., Kudo, S., Kitajima, Y., Harada, H., Furukawa, K., Matsuzaki, H., Emi, M., Nakabeppu, Y., Miyazaki, K., Sekiguchi, M., and Mukai, T. Silencing effect of CpG island hypermethylation and histone modifications on O6-methylguanine-DNA methyltransferase (MGMT) gene expression in human cancer. *Oncogene 22*, 55 (2003).

[22] Nguyen, N., Redfield, J., Ballo, M., Michael, M., Sorenson, J., Dibaba, D., Wan, J., Ramos, G. D., and Pandey, M. Identifying the optimal cutoff point for MGMT promoter methylation status in glioblastoma. *CNS Oncology 10*, 3 (2021).

[23] Ostrom, Q. T., Patil, N., Cioffi, G., Waite, K., Kruchko, C., and Barnholtz-Sloan, J. S. CBTRUS statistical report: Primary brain and other central nervous system tumors diagnosed in the United States in 2013-2017. *Neuro-Oncology 22*, Supplement_1 (10 2020), IV1–IV96.

[24] Patel, A., Dogan, H., Payne, A., Krause, E., Sievers, P., Schoebe, N., Schrimpf, D., Blume, C., Stichel, D., Holmes, N., Euskirchen, P., Hench, J., Frank, S., Rosenstiel-Goidts, V., Ratliff, M., Etminan, N., Unterberg, A., Dieterich, C., Herold-Mende, C., Pfister, S. M., Wick, W., Loose, M., von Deimling, A., Sill, M., Jones, D. T., Schlesner, M., and Sahm, F. Rapid-CNS2: rapid comprehensive adaptive nanopore-sequencing of CNS tumors, a proof-of-concept study. *Acta neuropathologica 143*, 5 (5 2022), 609–612.

[25] Payne, A., Holmes, N., Clarke, T., Munro, R., Debebe, B., and Loose, M. Nanopore adaptive sequencing for mixed samples, whole exome capture and targeted panels. *bioRxiv* (2020).

[26] Quillien, V., Lavenu, A., Ducray, F., Meyronet, D., Chinot, O., Fina, F., Sanson, M., Carpentier, C., Karayan-Tapon, L., Rivet, P., Entz-Werle, N., Legrain, M., Zalcman, E. L., Levallet, G., Escande, F., Ramirez, C., Chiforeanu, D., Vauleon, E., and Figarella-Branger, D. Clinical validation of the CE-IVD marked Therascreen MGMT kit in a cohort of glioblastoma patients. *Cancer Biomarkers 20*, 4 (2017).

[27] Quillien, V., Lavenu, A., Karayan-Tapon, L., Carpentier, C., Labussiäre, M., Lesimple, T., Chinot, O., Wager, M., Honnorat, J., Saikali, S., Fina, F., Sanson, M., and Figarella-Branger, D. Comparative assessment of 5 methods (methylation-specific polymerase chain reaction, methylight, pyrosequencing, methylation-sensitive high-resolution melting, and immunohistochemistry) to analyze O6-methylguanine-DNA- methyltranferase in a series of 100 glioblastoma patients. *Cancer 118*, 17 (2012).

[28] Radke, J., Koch, A., Pritsch, F., Schumann, E., Misch, M., Hempt, C., Lenz, K., Löbel, F., Paschereit, F., Heppner, F. L., Vajkoczy, P., Koll, R., and Onken, J. Predictive MGMT status in a homogeneous cohort of IDH wildtype glioblastoma patients. *Acta neuropathologica communications 7*, 1 (2019).

[29] Sahm, F., Brandner, S., Bertero, L., Capper, D., French, P. J., Figarella-Branger, D., Giangaspero, F., Haberler, C., Hegi, M. E., Kristensen, B. W., Kurian, K. M., Preusser, M., Tops, B. B. J., van den Bent, M., Wick, W., Reifenberger, G., and Wesseling, P. Molecular diagnostic tools for the World Health Organization (WHO) 2021 classification of gliomas, glioneuronal and neuronal tumors; an EANO guideline. *Neuro-oncology* (6 2023).

[30] Siller, S., Lauseker, M., Karschnia, P., Niyazi, M., Eigenbrod, S., Giese, A., and Tonn, J. C. The number of methylated CpG sites within the MGMT promoter region linearly correlates with outcome in glioblastoma receiving alkylating agents. *Acta neuropathologica communications 9*, 1 (3 2021), 35.

[31] Stupp, R., Taillibert, S., Kanner, A., Read, W., Steinberg, D. M., Lhermitte, B., Toms, S., Idbaih, A., Ahluwalia, M. S., Fink, K., Di Meco, F., Lieberman, F., Zhu, J. J., Stragliotto, G., Tran, D. D., Brem, S., Hottinger, A. F., Kirson, E. D., Lavy-Shahaf, G., Weinberg, U., Kim, C. Y., Paek, S. H., Nicholas, G., Burna, J., Hirte, H., Weller, M., Palti, Y., Hegi, M. E., and Ram, Z. Effect of tumor-treating fields plus maintenance temozolomide vs maintenance temozolomide alone on survival in patients with glioblastoma a randomized clinical trial. *JAMA - Journal*

of the American Medical Association 318, 23 (2017).

[32] Tierling, S., Jürgens-Wemheuer, W. M., Leismann, A., Becker-Kettern, J., Scherer, M., Wrede, A., Breuskin, D., Urbschat, S., Sippl, C., Oertel, J., Schulz-Schaeffer, W. J., and Walter, J. Bisulfite profiling of the MGMT promoter and comparison with routine testing in glioblastoma diagnostics. *Clinical Epigenetics 14*, 1 (2022).

[33] Torre, M., Wen, P. Y., and Iorgulescu, J. B. The predictive value of partial MGMT promoter methylation for IDH-wild-type glioblastoma patients . *Neuro-Oncology Practice* (2022).

[34] Wenger, A., Vega, S. F., Kling, T., Bontell, T. O., Jakola, A. S., and Carén, H. Intratumor DNA methylation heterogeneity in glioblastoma: implications for DNA methylation-based classification. *Neuro-Oncology 21*, 5 (5 2019), 616.

[35] Wongsurawat, T., Jenjaroenpun, P., De Loose, A., Alkam, D., Ussery, D. W., Nookaew, I., Leung, Y. K., Ho, S. M., Day, J. D., and Rodriguez, A. A novel Cas9-targeted long-read assay for simultaneous detection of IDH1/2 mutations and clinically relevant MGMT methylation in fresh biopsies of diffuse glioma. *Acta Neuropathologica Communications 8*, 1 (6 2020), 1–13.

[36] Xie, H., Tubbs, R., and Yang, B. Detection of MGMT promoter methylation in glioblastoma using pyrosequencing. *International Journal of Clinical and Experimental Pathology 8*, 2 (2015).

[37] Yuan, G., Niu, L., Zhang, Y., Wang, X., Ma, K., Yin, H., Dai, J., Zhou, W., and Pan, Y. Defining optimal cutoff value of MGMT promoter methylation by ROC analysis for clinical setting in glioblastoma patients. *Journal of Neuro-Oncology 133*, 1 (2017).

[38] Zhang, J., F.G. Stevens, M., and D. Bradshaw, T. Temozolomide: Mechanisms of Action, Repair and Resistance. *Current Molecular Pharmacology 5*, 1 (2011).

Supplementary material

Table 1: Summary of samples included in this study.

	Prospective nCats	Retrospective nCats	Rapid-CNS	Total
Glioblastoma, IDHwt	13	29	49	**91**
Meningioma	0	12	0	**12**
Astrocytoma, HG, IDHmut	0	4	4	**8**
Oligodendroglioma, IDHmut	0	2	6	**8**
Astrocytoma, IDHmut	3	1	3	**7**
Metastasis	0	7	0	**7**
Pilocytic astrocytoma	0	0	4	**4**
Medulloblastoma	0	2	0	**2**
Lymphoma	0	2	0	**2**
Pleomorphic xanthoastrocytoma	0	2	0	**2**
Atypical teratoid/rhabdoid tumor	0	0	1	**1**
CNS Neuroblastoma	0	1	0	**1**
Ependymoma	0	1	0	**1**
Ganglioglioma	0	1	0	**1**
Hemangiopericytoma	0	1	0	**1**
Total	**16**	**65**	**67**	**148**

Table 2: Summary of reported optimal cut-offs for determining methylated versus unmethylated samples

Author	Year	Method	Patients	CpGs	Optimal cut-off	Comment	Reference
Hegi	2019	qMSP	4041		>1.27	"Grey-zone" patients benefit from TMZ	[13]
Johannessen	2018	qMSP, PSQ	48		7 %	PSQ gives better results than other methods	[17]
Nguyen	2021	PSQ	109		21 %	Higher methylation corrilates with longer OS	[22]
Quillien	2012	MSP, PSQ, MS-HRM	100	5	8 %	PSQ performs best	[27]
Xie	2015	PSQ	43		10 %	Not testing cut-off	[36]
Yuan	2017	PSQ	84	4	12.50 %	Higher methylation corrilates with longer OS	[37]
Brigliadori	2016	PSQ	105	10	30 %	"Grey-zone" patients do not benefit from TMZ	[4]
Radke	2019	PSQ, sqMSP	111		10 %	Best results when PSQ and MSP were combined	[28]
Chai	2021	PSQ	173	4	10 %	*MGMT* promoter methylation has predictive value in IDH-mutant glioblastoma	[5]
Dovek	2019	qMSP	165		>1	"Grey-zone" patients benefit from TMZ, higher methylation does not correlate with longer OS	[7]
Siller	2021	MSP, Sseq	215	25		Linear correlation between number of methylated CpG sites and OS	[30]